Supplementary Information – What chemical species are responsible for new particle formation and growth in the Netherlands? A hybrid positive matrix factorization (PMF) analysis using aerosol composition (ACSM) and size (SMPS)

S1. Figures and tables

Table of Figures

Table of Tables

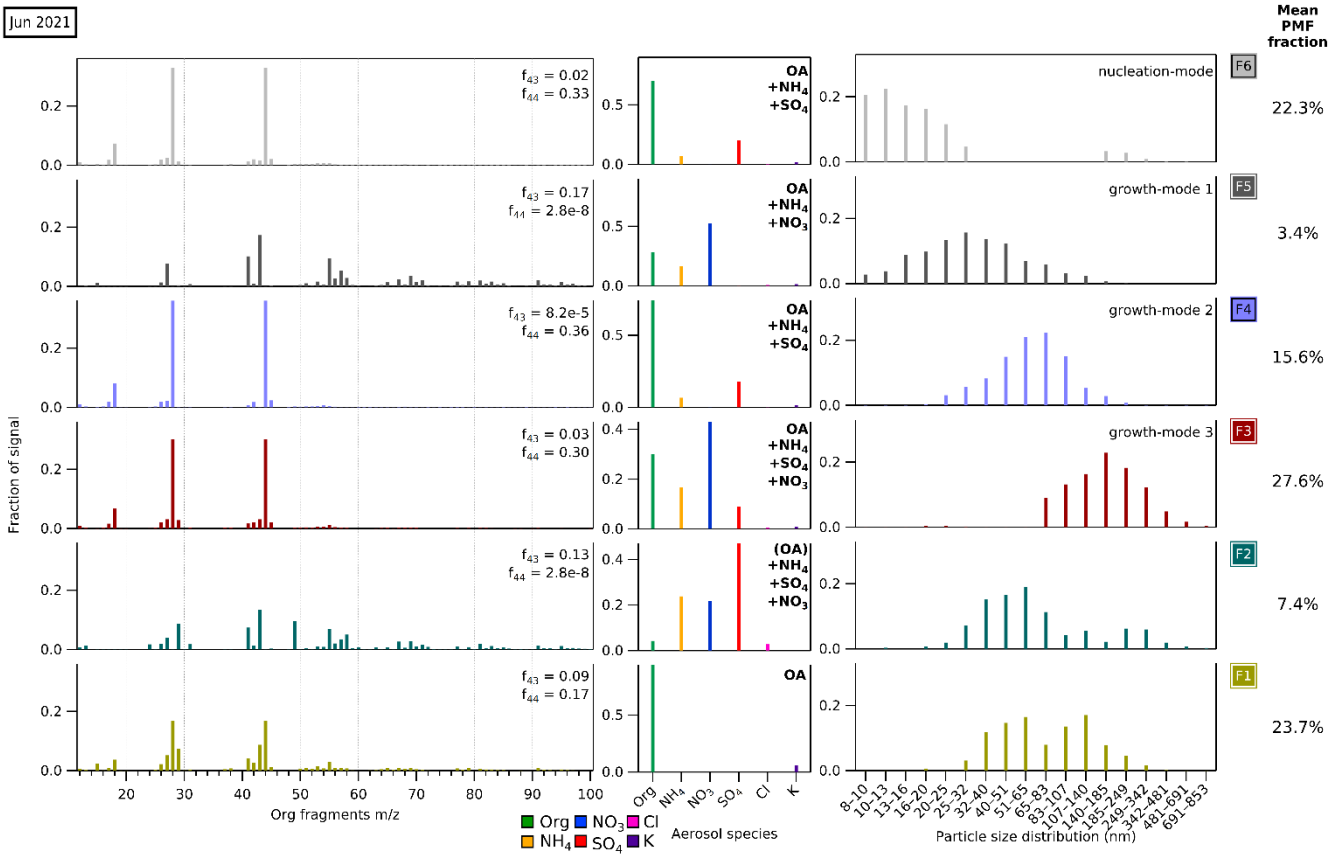

Figure S1. The profiles of 6-factor solution from the combined ACSM-SMPS dataset in June 2021. Each factor is split into three matrices with their own signal fraction axes. The lefthand panel shows the organic fragment mass spectrum profiles from ACSM. The values of f_{44} (CO_2^+ fragment) representing higher oxidation level and f_{43} (CH_3CO^+ and $C_3H_7^+$) representing lower oxidation level are given. The middle panel shows the ACSM standard aerosol species concentrations (organics (Org), ammonium (NH_4), nitrate (NO_3), sulfate (SO_4), chloride (Cl), and potassium (K)). The righthand panel shows the particle size distribution profiles from the SMPS. The mean PMF fractions are shown to the right, indicating the mean contribution of each hybrid PMF factor to the "total variable reconstruction" by PMF throughout the period (note we have reordered factors to be consistent across the 3 months). The factors in May 2021 are assigned as: (F1) OA, (F2) (OA)+NH_4+SO_4+NO_3, (F3) growth-mode 3 OA+NH_4+SO_4+NO_3, (F4) growth-mode 2 OA+NH_4+SO_4, (F5) growth-mode 1 OA+NH_4+NO_3, and (F6) nucleation-mode OA+NH_4+SO_4. Factors with OA listed inside parentheses indicates OA below 25% of the total mass.

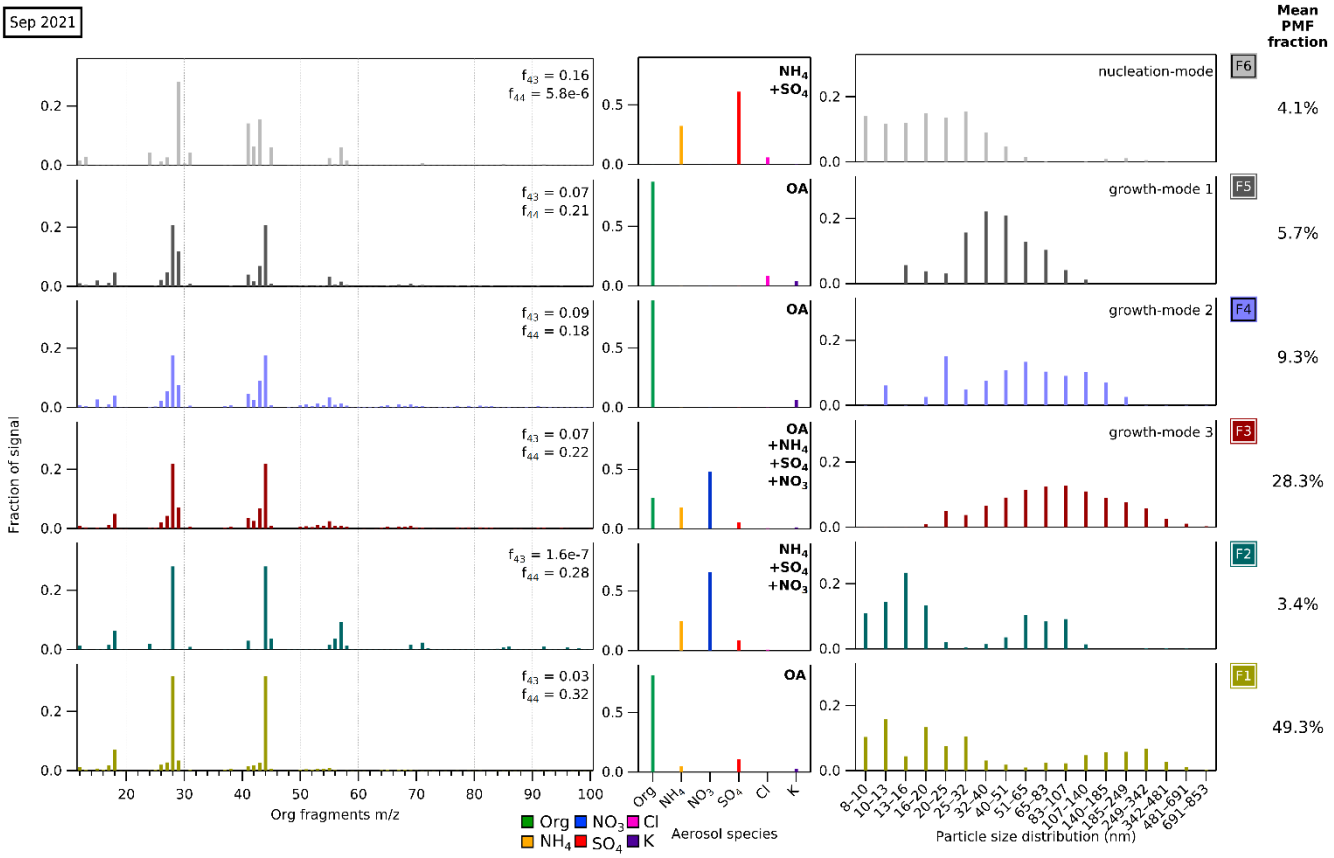

Figure S2. The profiles of 6-factor solution from the combined ACSM-SMPS dataset in September 2021. Each factor is split into three matrices with their own signal fraction axes. The lefthand panel shows the organic fragment mass spectrum profiles from ACSM. The values of f_{44} (CO_2^+ fragment) representing higher oxidation level and f_{43} (CH_3CO^+ and $C_3H_7^+$) representing lower oxidation level are given. The middle panel shows the ACSM standard aerosol species concentrations (organics (Org), ammonium (NH_4), nitrate (NO_3), sulfate (SO_4), chloride (Cl), and potassium (K)). The righthand panel shows the particle size distribution profiles from the SMPS. The mean PMF fractions are shown to the right, indicating the mean contribution of each hybrid PMF factor to the "total variable reconstruction" by PMF throughout the period (note we have reordered factors to be consistent across the 3 months). The factors in May 2021 are assigned as: (F1) OA, (F2) NH_4+SO_4+NO_3, (F3) growth-mode 3 OA+NH_4+NO_3, (F4) growth-mode 2 (OA)+NH_4+SO_4, (F5) growth-mode 1 OA, and (F6) nucleation-mode (OA)+NH_4+SO_4. Factors with OA listed inside parentheses indicates OA below 25% of the total mass. Some factor profiles may have organic fragments mass spectrum despite negligible or no ACSM organic composition (Org) variable contribution. We interpret these fragments showing the profile of trace OA that is insufficient to result in a significant contribution of the Org variable.

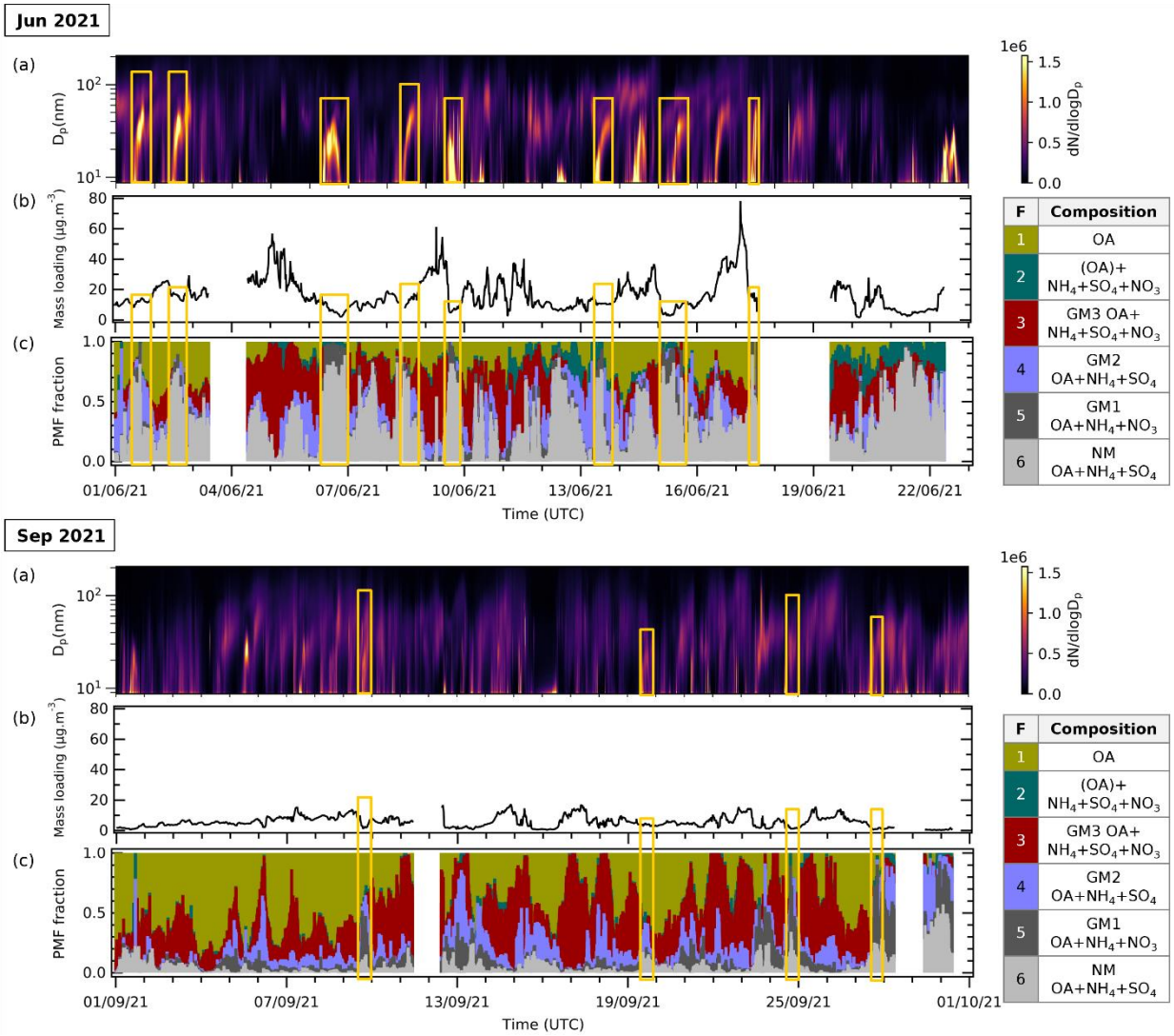

Figure S3. Time series of (a) particle size distribution (dN/dlogD_p) in cm^{-3} with logarithmic scale in particle size obtained from SMPS measurements, (b) total mass loading calculated from ACSM species concentration (using Tofware) in µg.m^{-3}, and (c) reconstructed PMF fraction (stacked) from analyses in June and September 2021. Orange outlined sections indicate periods during which high episodes of size-driven factors are observed. These episodes coincide with relatively low total aerosol mass conditions and high fine particle concentrations.

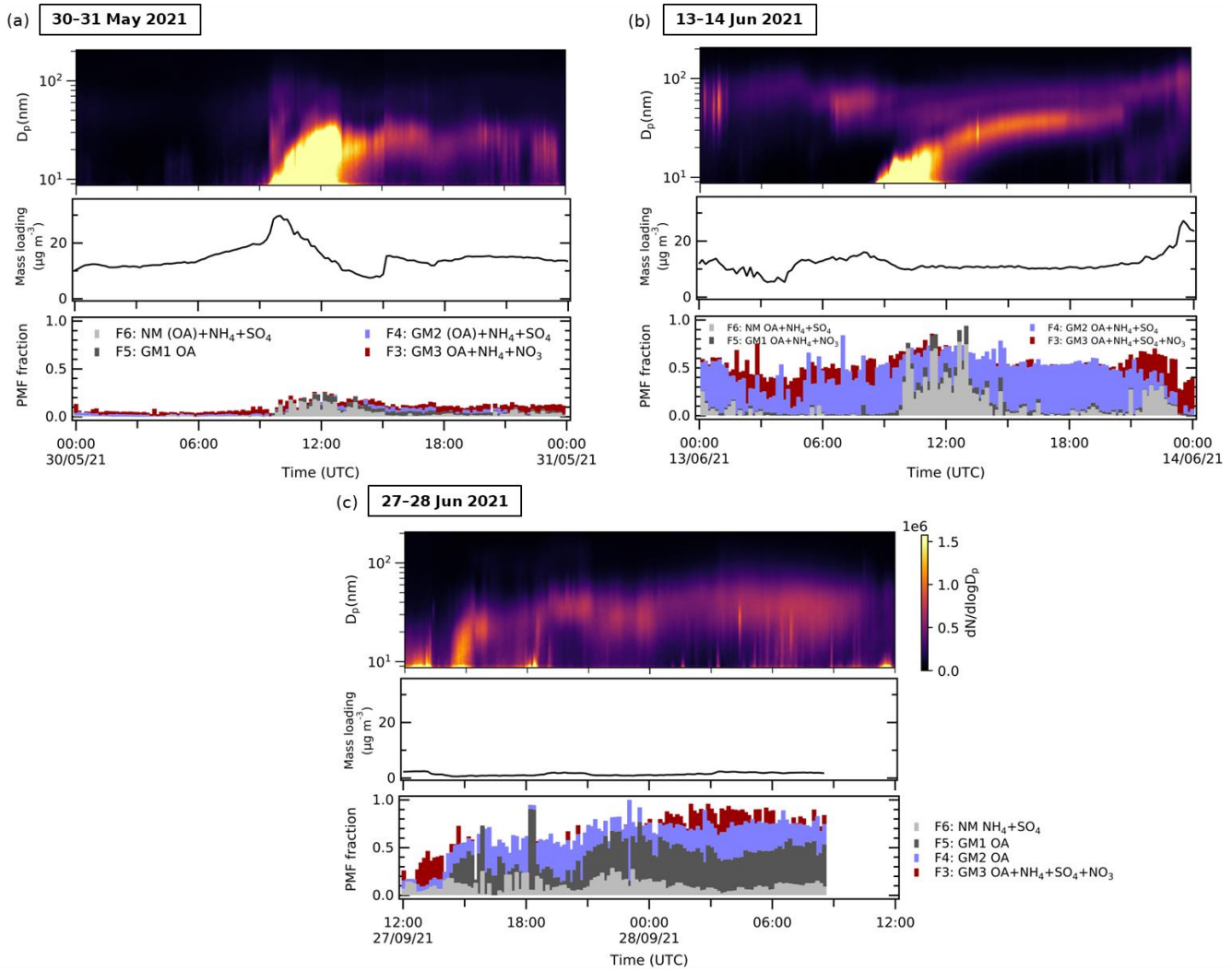

900

Figure S4. Selected timeseries windows during which new particle formation (NPF) events were detected by the scanning mobility particle sizer (SMPS) resembling 'banana' shapes at (a) 30 May 2021 00:00 to 31 May 2021 00:00 UTC, (b) 13 Jun 2021 00:00 to 14 Jun 2021 00:00 UTC, and (c) 27 Sep 2021 12:00 to 28 Sep 2021 12:00 UTC. Rapid increases of fine new particles were observed. During these events, the increase in size-driven factors F7 and F6 can be seen equally in the reconstructed PMF fraction time series.

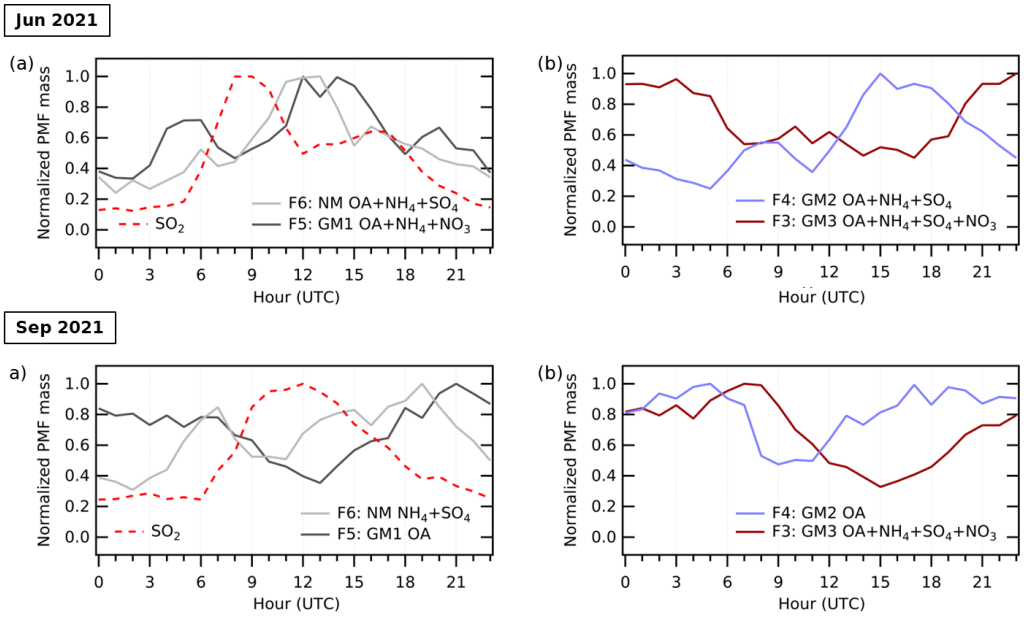

905

Figure S5. Normalized diurnal cycles in June and September 2021 of (a) the size-driven factors of F6 and F5, and SO_2 as the sulfate precursor, and (b) the size-driven factors of F4 and F3. Notice that from F6 to F3, the factors' diurnal pattern shifted from high daytime to high nighttime concentration.

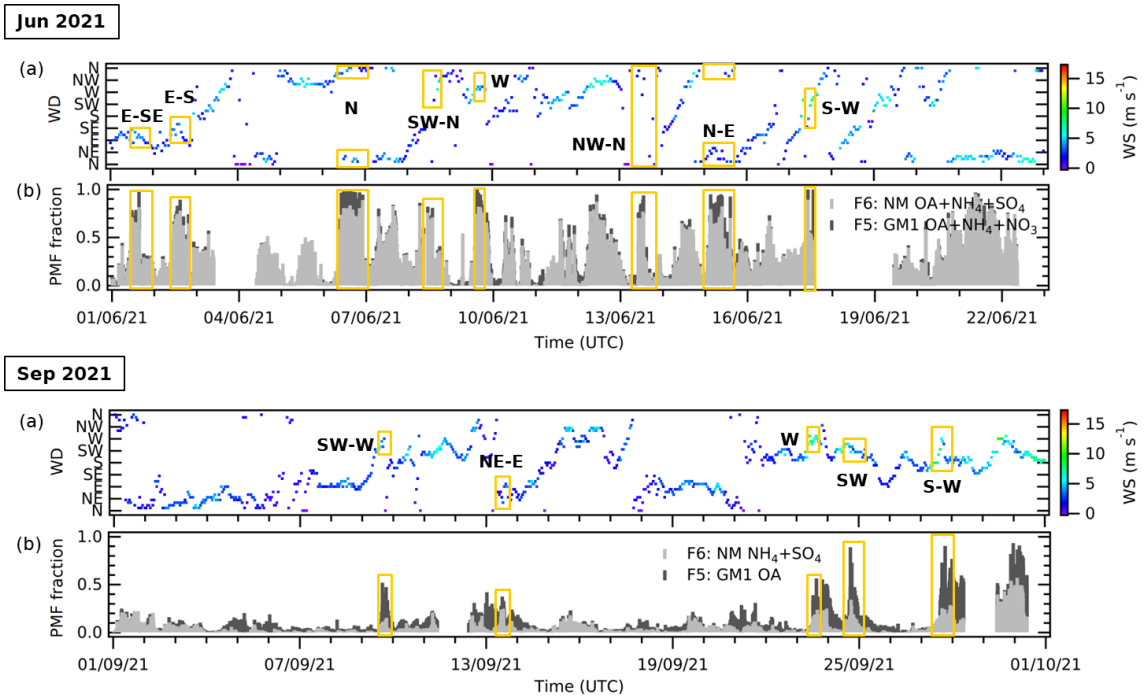

910 **Figure S6**. Timeseries of (a) wind direction (WD) color-coded with wind speed (WS), and (b) reconstructed PMF fractions F6 and F5 (stacked) corresponding to nucleation-mode and first growth-mode particles in June and September 2021. Orange outlined sections indicate high F6 and F5 episodes. We can observe that new particle formation is correlated with air masses from the southwesterly-westerly sector or northerly-easterly sector.

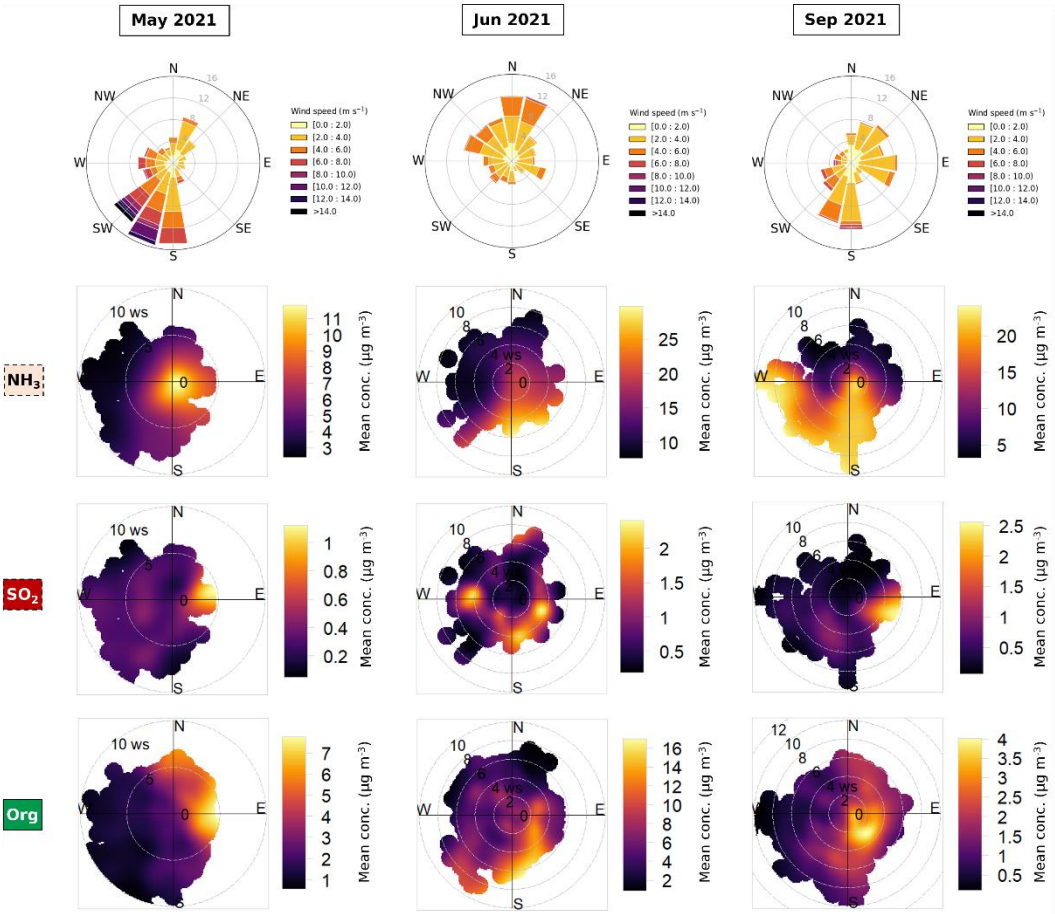

915 **Figure S7.** Wind roses and bivariate polar plots of nucleation-mode particle precursor concentrations by wind speed and wind direction measured in Cabauw in May, June, and September 2021. The species include ammonia (NH_3) and sulfur dioxide (SO_2) in the gaseous phase in hourly resolution, and organics (Org) in the aerosol phase in 10-minute resolution. NH_3 is predominant around the site, particularly from the southern sector. SO_2 is prevalent from the east and west of the site. Org species are predominantly coming from the eastern sector explaining the correlation of nucleation-mode factor (F6) episodes with easterlies in May and June 2021 when OA participates in early NPF.

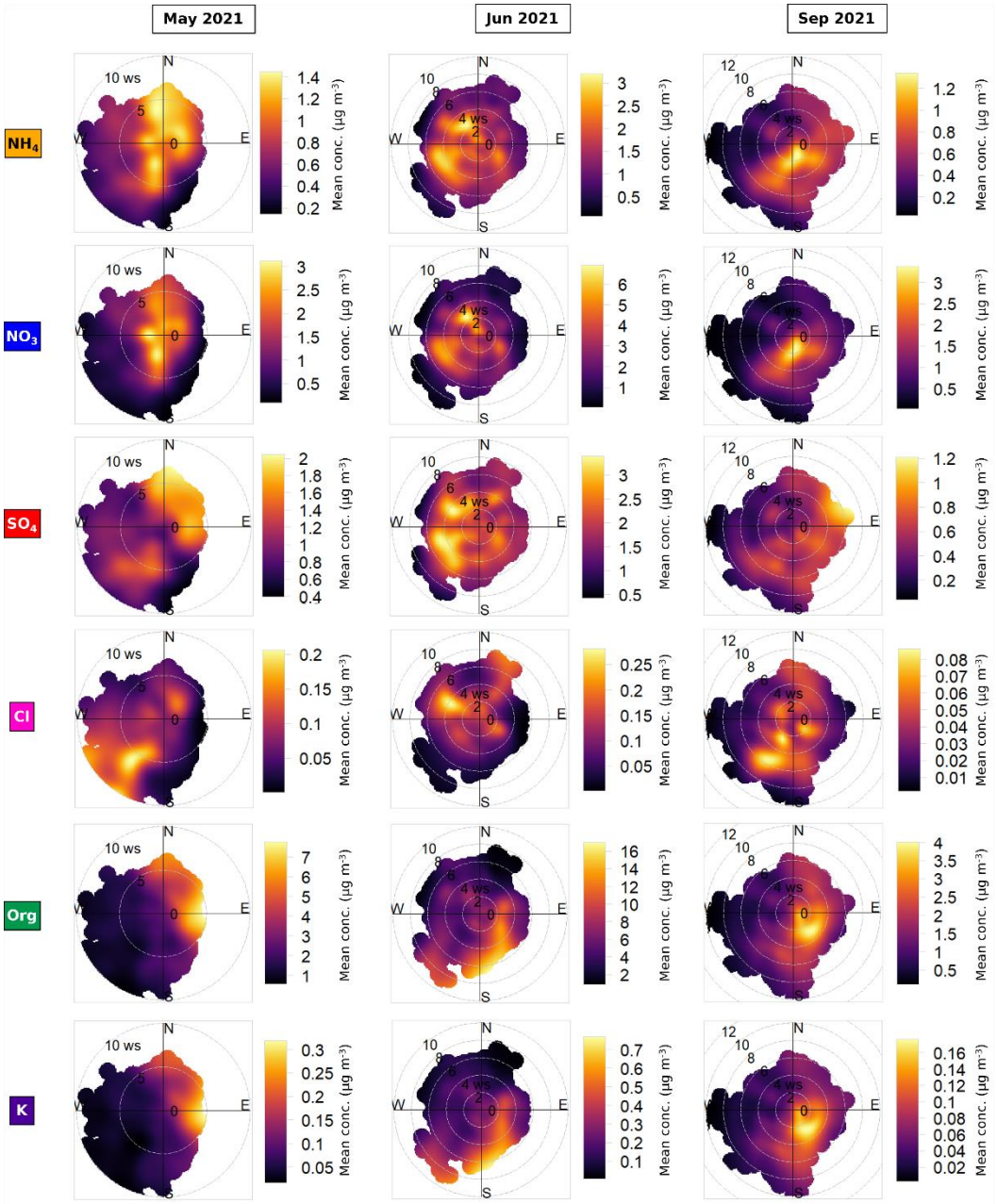

Figure S8. Wind roses and bivariate polar plots of ACSM-generated chemical species by wind speed and wind direction measured in Cabauw in May, June, and September 2021. The species include ammonium (NH_4), nitrate (NO_3), sulfate (SO_4), chloride (Cl), organics (Org), and potassium (K) in 10-minute resolution. NO_3 and SO_4 are found to be correlated to NH_3 source direction (see Fig. S7). across seasons due to formation of ammonium nitrate and sulfate. NO_3 are correlated with the southern and western sector of the site. SO_4 is correlated to westerlies and north-easterlies, influenced by both NH_3 and SO_2 source direction since they react forming ammonium sulfate (see Fig. S7). As trace ions, Cl is correlated with SO_4, while K is correlated with Org.

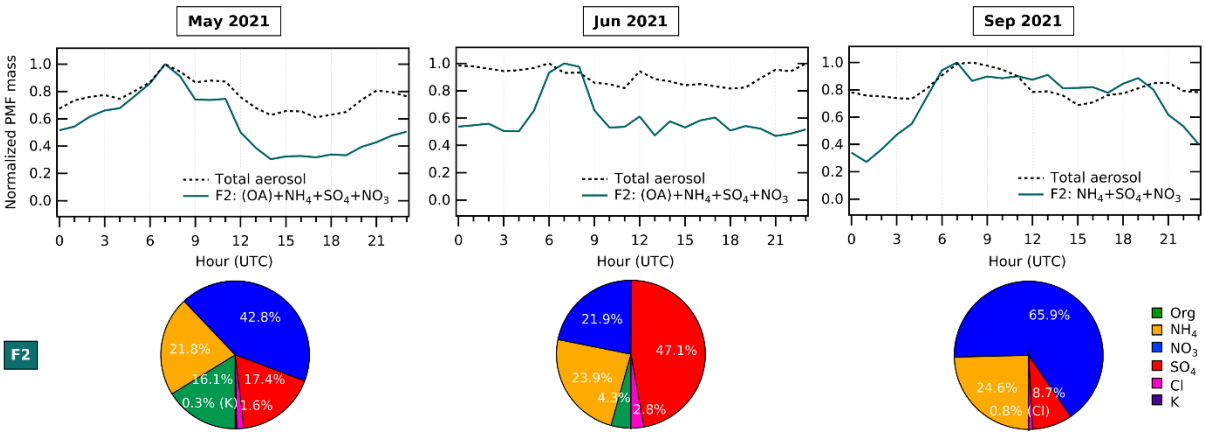

Figure S9. Diurnal cycles of F2 and total aerosol mass loading measured by the ACSM (top) with associated composition (bottom) across periods. F2 has a higher daytime value that resembles the diurnal cycle of total aerosol concentration except in summer (June).

S2. Determining composition regimes from bulk atmospheric composition

The ion balance ratio ($n_{NH_4}/(n_{NO_3}+2\times n_{SO_4}+n_{Cl})$) is used to assess the ion-pairing between cations and anions forming inorganic aerosol (IA). Ambient aerosol is normally charge-balanced, meaning that the major cation (NH_4^+) and anion species (NO_3^-, SO_4^{2-}, and Cl^-) should have one-to-one molar ratio. To calculate the ion balance ratio, we compare the measured ammonium molar concentration (n_{NH_4}) to the total ammonium needed to neutralize the measured major anion concentration ($n_{NO_3}+2\times n_{SO_4}+n_{Cl}$). In spring (May), the ion balance is 0.99 which can be regarded as unity, meaning that the ion charge is fully neutralized. In summer (June), the ion balance ratio is less than unity (0.98). This may be caused by aerosol acidity (Farmer et al., 2010; Docherty et al., 2011) with excess in H^+ aerosol being undetected by the instrument. Alternatively, nitrate or sulfate may be present in compounds other than ammonium salts. They can form salts with undetected cations (e.g., $NaNO_3$, Na_2SO_4, $Ca(NO_3)_2$), or exist in form of organic nitrates and organic sulfates, yielding an additional amount of nominal nitrate and sulfate detected by ACSM (Farmer et al., 2010; Docherty et al., 2011). The ion balance ratio in autumn (September) is larger than unity (1.08). This can arise from uncharged amines detected as ammonium by the ACSM (Farmer et al., 2010; Docherty et al., 2011), or from the presence of unmeasured anions such as carboxylates.

The aerosol species excess for each period can be deduced from the aerosol formation chemistry in a HNO_3-NH_3-H_2SO_4-H_2O system (Ansari and Pandis, 1998; Seinfeld and Pandis, 2016; Tsai et al., 2016). When the molar ratio of free ammonia-to-sulfate total is larger than two, NH_3 prefers to react homogeneously with H_2SO_4 to form ammonium sulfate ($(NH_4)_2SO_4$). The rest of NH_3 will react with HNO_3 to form ammonium nitrate (NH_4NO_3) (Ansari and Pandis, 1998). The surplus is calculated based on the assumption that all available sulfate reacts with ammonia first to form $(NH_4)_2SO_4$. The remaining NH_3 forms NH_4NO_3 with nitrate and can result in either ammonium or an overabundance of nitrate.

In summer (June), we observe roughly a doubling in aerosol concentration for all IA and an increase with a factor 2.6 in OA compared to May. This increase is mainly due to increasing anthropogenic activities, photosynthesis, and evapotranspiration of plants in summer. However, a mean nitrate excess is still observed ($n_{NH_4}/(n_{NO_3}+2\times n_{SO_4}+n_{Cl}) < 1$). In autumn (September), the particle concentrations decrease again, with a relatively larger decrease for sulfate. The discrepancy between the decrease of sulfate and other IA species concentrations in September leads to a change in ion balance ratio, generating the ammonium excess discussed previously ($n_{NH_4}/(n_{NO_3}+2\times n_{SO_4}+n_{Cl}) > 1$). In addition, to illustrate how the concentration of sulfate relates to nitrate, we introduce the mean sulfate-to-nitrate molar concentration ratio (n_{SO_4}/n_{NO_3}). The values of n_{SO_4}/n_{NO_3} in May, June, and September were 0.41, 0.43, and 0.23 respectively (see summary in Table S1). A lower n_{SO_4}/n_{NO_3} as found in autumn (September) suggests a more sulfate-poor regime, while a higher n_{SO_4}/n_{NO_3} in spring (May) and summer (June) indicates a more sulfate-rich composition.

Besides the two previous ratios, the mean organic-to-ammonium mass ratio (m_{Org}/m_{NH_4}) is used to indirectly compare the composition of IA and OA of factors across periods. Ammonium is a good representation of IA, as ammonium salts are the dominant inorganic species in the atmosphere. A mass ratio (m_{Org}/m_{NH_4}) is used instead of molar ratio because organic species are measured as a mixture of various organic compounds by ToF-ACSM. The m_{Org}/m_{NH_4} values in May, June, and September were 2.47, 3.36, and 2.90, respectively (see summary in Table S1). The higher value observed in June implies an organic-rich regime, while the other months are in a more inorganic regime.

Table S1. Mean bulk atmospheric chemical composition in the three period as detected by the ToF-ACSM and collocated gas measurements in Cabauw. The ion balance ratio ($n_{NH_4}/(n_{NO_3}+2\times n_{SO_4}+n_{Cl})$) was unity in May, less than unity in June, and more than unity in September. An overabundance of nitrate was found in May and June, while ammonium excess is found in September.

Species/ratio	Mean concentration in May 2021 (spring)		Mean concentration in Jun 2021 (summer)		Mean concentration in Sep 2021 (autumn)	
	Mass ($\mu g\ m^{-3}$)	Molar (10^{-4} mol m^{-3})	Mass ($\mu g\ m^{-3}$)	Molar (10^{-4} mol m^{-3})	Mass ($\mu g\ m^{-3}$)	Molar (10^{-4} mol m^{-3})
NH_3*	7.03	41.37	15.25	89.56	12.67	74.37
NO_x	9.55	21.79	10.90	24.90	14.78	34.08
SO_2	0.34	0.54	0.85	1.33	0.59	0.91
Org	2.49	-	6.37	-	2.14	-
NO_3^-	1.84	2.97	3.42	**5.52****	1.57	2.53
NH_4^+	1.01	5.61	1.90	10.54	0.74	**4.10****
SO_4^{2-}	1.15	1.20 (×2 = 2.40)	2.29	2.39 (×2 = 4.78)	0.55	0.57 (×2 = 1.14)
Cl^-	0.11	0.30	0.15	0.42	0.05	0.13
K^+	0.08	0.21	0.23	0.58	0.09	0.23
$n_{NH_4}/(n_{NO_3}+2\times n_{SO_4}+n_{Cl})$***	-	0.99	-	0.98	-	1.08
n_{SO_4}/n_{NO_3}	-	0.41	-	0.43	-	0.23
m_{Org}/m_{NH_4}	2.47	-	3.36	-	2.90	-
Composition regime	sulfate-rich		nitrate excess, organic- and sulfate-rich		ammonium excess, sulfate-poor	

* Data taken from Zegveld-Oude Meije measurement station

**Aerosol species that are found having excess quantity

***Ion balance ratio is the ratio between the measured ammonium (n_{NH_4}) and the total ammonium needed to neutralize the major anions ($n_{NO_3}+2\times n_{SO_4}+n_{Cl}$). The value is obtained from linear regression.

S3. F1: Background OA factor

There are two distinct profiles of F1, affected by seasonality of organic-rich regime and meteorological variables. In the organic-rich regime during summer (June), this factor consists almost solely of organics (94.1%) with trace potassium (5.8%). In spring (May) and autumn (September), there is less organic (81.2% to 83.5%), again traces of potassium (2.6% to 3.3%), and more significant contributions of ammonium (3.3% to 5.1%) and sulfate (10.0% to 11.1%).

In spring (May) and autumn (September), F1 exhibits a diurnal pattern consistent with a more oxidized oxygenated organic aerosol (MO-OOA) factor, with concentration rising slightly across the day (see Fig. S10). The f_{44} values are 0.28 and 0.32 in spring (May) and autumn (September), respectively. MO-OOA has a relatively stable concentration throughout the day because the factor is typically part of a long-range transported aerosol (Kodros et al., 2020; Chen et al., 2022). The concentration slightly increases from morning to afternoon due to photochemical oxidation. The factor then shows a slight decrease in the late night until sunrise, as its production slows in the absence of radiation. This profile was found in airmasses arriving from the easterly sector that extends from northerly (0°) to southerly-southeasterly (157.5°) (see Fig. S10), making up 42.1% to 49.3% of total reconstructed PMF mass. To the east, the province of Gelderland is mostly covered by agricultural grass land and forested protected nature areas that emit VOCs, therefore increasing the amount of OA produced. Easterly wind directions may also contain the accumulated pollutants or VOCs from continental Europe, and therefore may contain a variety of OA from either biogenic or anthropogenic sources.

Meanwhile, in summer (June), F1 resembles more the description of less oxidized oxygenated organic aerosol (LO-OOA) factor (see Fig. S10). The f_{43} and f_{44} values are 0.09 and 0.17, respectively. LO-OOA has higher nighttime concentration with a slight decrease during the day, suggesting more regional source and higher partitioning of organic vapors into the aerosol phase in the shallow nocturnal boundary layer (Chen et al., 2022). The source region of the organic aerosol is more correlated

to wind from the southern sector, extending from northeasterly to southwesterly (45° to 225°) (see Fig. S10). By comparing to other factors in the same month and F1 across season, we suggest that due to organic-rich regime, high mean radiation, and high temperatures, highly oxidized organic compounds participate substantially in the size-driven factors forming new particles. This results in less aged OA (lower f_{44} value) in F1 and F2, and a reduction in the overall PMF fraction of F1 (accounting only 23.7% of total reconstructed PMF mass).

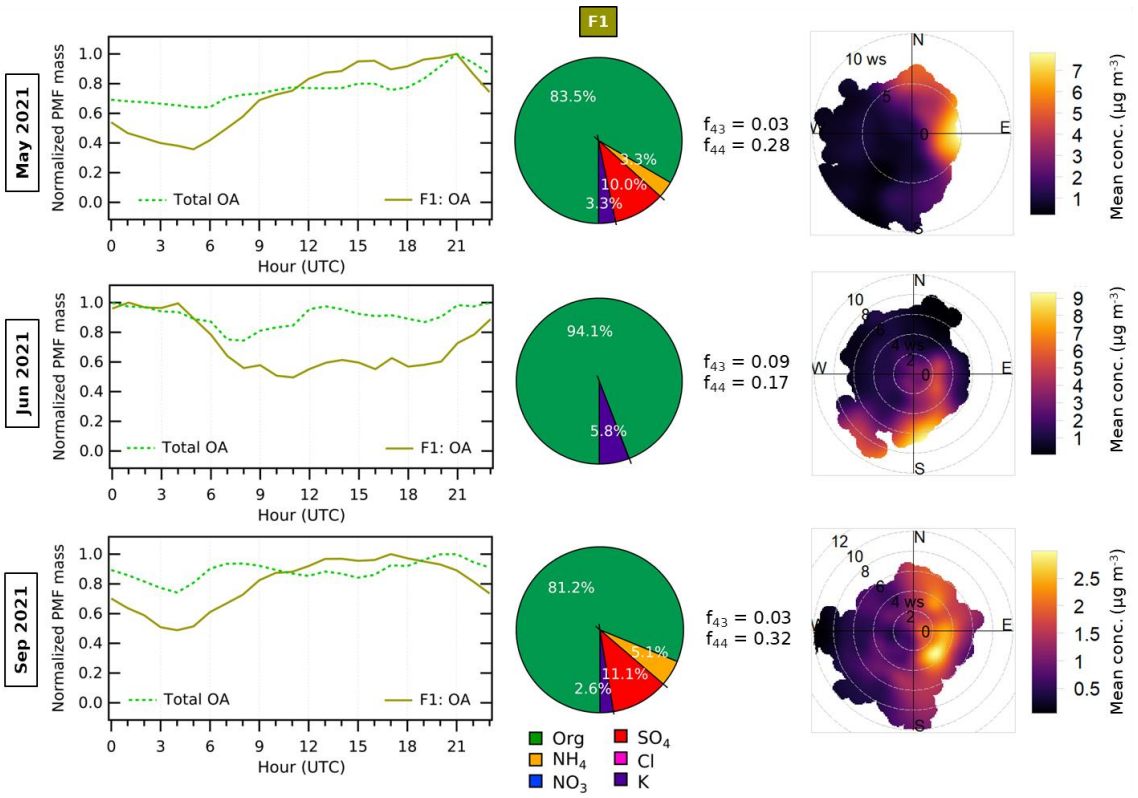

Figure S10. Diurnal cycles of F1 and total OA measured by ACSM in May, June, and September 2021 are shown (left), with associated composition (middle) and bivariate polar plots of F1 concentration by wind speed and direction (right) in 10-minute resolution. The concentrations increase slightly during the day due to photochemical activity and then concentrated in the boundary layer after sunset. It decreases around the midnight until morning due to absence of photochemistry. The OA F1 plumes mostly arrive from the eastern and northern sector in Cabauw.

S4. Correlation of chloride-sulfate and potassium-organic species

Chloride (Cl) and potassium (K) generally only contribute a trace amount of mass in the aerosol (see Fig. 3, Fig. S1, and Fig. S2). Nonetheless, source apportionment of ACSM species and PMF factors showed some interesting patterns with chloride and potassium species. Most of the time, chloride is a visible minority to factors that are abundant in sulfate. In nucleation-mode F6, which is mostly composed of ammonium sulfate, a trace of chloride (0.1% to 6.0%) can be found. Such appearance is also observed for the sulfate-containing size-driven factors (i.e., F4 in May, F3 in June, and F3 in September), where chloride is 0.6% to 3.6% of the total factor mass. The chloride across periods may arrive from sea salt aerosols, although its sources varied as seen in Fig. S8. This is broadly consistent with the dominant source of sulfate being the port region, where sea spray can be a source of the co-occurring chloride.

A trace amount of potassium was frequently found on factors related to OA. When the OA in F6 is higher during summer (June), a significant amount potassium (2.1%) can be found in the factor. This appearance can also be observed in factors that are dominated by OA or in OA+IA mixed factors (e.g., F5, some F4, F3, and F1) where the potassium concentration ranges from 0.8% to 6.2% of the total mass. Such correlation was also confirmed by the similar pollution rose of the ACSM organic and potassium species (see Fig. S8). This suggests that the potassium originated from the same source as the emissions of

organic compounds, perhaps indicative of a woodsmoke contribution from biomass burning (Pio et al., 2008; Urban et al., 2012; Pachon et al., 2013).